Current Opinion in Solid State and Materials Science 15 (2011) 106–115

Contents lists available at ScienceDirect

Current Opinion in Solid State and Materials Science

journal homepage: www.elsevier.com/locate/cossms

Phase field modeling of microstructure evolution in steels

Matthias Militzer *

The Centre for Metallurgical Process Engineering, The University of British Columbia, Vancouver, BC, Canada V6T 1Z4

ARTICLE INFO

Article history:
Available online 20 October 2010

Keywords:
Phase field modeling
Austenite decomposition
Austenite formation
Ferrite
Pearlite
Grain growth
Recrystallization
Heat affected zone

ABSTRACT

This article provides an overview on the application of phase field models to describe microstructure evolution in steels. The focus will be on phase field modeling of the austenite–ferrite transformation as this has emerged as a particularly active area of research in the past few years. Phase field models are powerful tools to deal with the complex morphologies, e.g. Widmanstätten ferrite, that may result from these transformations. Even though much progress has been attained there is still significant work to be done in applying these models to processing of advanced steels with complex multi-phase microstructures. In particular, the phase field approach promises to have significant impact on modeling of bainite formation and the microstructure evolution in the heat affected zone of welds.

1. Introduction

The phase field model (PFM) approach has increasingly been used over the past decade to model microstructure evolution in steels. Initially, PFMs were used to simulate solidification but more recently they have also been applied to solid–solid phase transformations [1]. The primary interest of these modeling efforts has been the austenite–ferrite transformation both austenite formation and austenite decomposition. Austenite decomposition is arguably the most widely studied phase transformation because of its practical importance as a metallurgical tool to tailor the properties of steels. To a lesser extent grain growth and recrystallization have also been considered. There is now also an increasing emphasis on using PFMs to simulate microstructure evolution in the heat affected zone (HAZ) of welds. This has stimulated research to explore the advantages of PFM in modeling microstructure evolution under spatial constraints, e.g. due to the steep temperature gradients in the HAZ. Even though there are a variety of PFM approaches available a significant body of the simulation work for steels has been conducted with a multi-phase field approach using the commercially available code MICRESS® (microstructure evolution simulation software) [2]. In the multi-phase field approach each grain and/or microstructure constituent is characterized by its own phase field parameter and can thus be tracked throughout the simulation to predict the evolution of an assembly of grains and phases. An advantage of MICRESS® is its versatility and ease of use for applications of the phase field method. Nevertheless, the application potential of PFMs is not restricted to this particular software and alternative PFM methods [3–6] have been applied to steel.

The present review first provides a brief survey of the phase field methodology and its application to steel. Subsequently, the status of the PFM application will be examined in more detail for austenite decomposition, austenite formation as well as recrystallization and grain growth with an emphasis on microstructure evolution in the HAZ. Finally, conclusions for future investigations will be proposed based on the presented analysis of the recent literature.

2. General survey

In the context of analyzing the strengths and limitations of the phase field methodology and its applications to steels it is useful to briefly recall the basics of this approach. As an example, the multi-phase field equations proposed by Steinbach et al. [7] are used as they provide an easy correlation with physical parameters (e.g. interface mobilities and energies). In this approach, each microstructure constituent, e.g. grain i, is prescribed by its own phase field parameter ϕ_i [$i = 1, \ldots, N$] where ϕ_i is equal to 1 inside grain i and 0 elsewhere. At the interface between two grains there is a gradual change of the two corresponding phase field parameters from 0 to 1 such that $\sum_i^N \phi_i(r,t) = 1$ holds at each position, r, in the simulation domain with a total number of N grains. The rate of change of the phase field parameters is given by a set of coupled differential equations [7]:

$$\frac{d\phi_i}{dt} = \sum_{i \neq j} \mu_{ij} \left[\sigma_{ij} \left\{ \phi_j \nabla^2 \phi_i - \phi_i \nabla^2 \phi_j + \frac{\pi^2}{2\eta_{ij}^2} (\phi_i - \phi_j) \right\} + \frac{\pi}{\eta_{ij}} \sqrt{\phi_i \phi_j} \Delta G_{ij} \right] \quad (1)$$

* Tel.: +1 604 8223676; fax: +1 604 8223619.
E-mail address: matthias.militzer@ubc.ca

1359-0286/$ - see front matter © 2010 Elsevier Ltd. All rights reserved.
doi:10.1016/j.cossms.2010.10.001

where μ_{ij} is the interface mobility, σ_{ij} is the interfacial energy, η_{ij} is the interface thickness and ΔG_{ij} is the driving pressure. The evolution of the phase field parameters describing the microstructure is governed by minimization of the total free energy of the system. The phase field equations can be coupled with the diffusion equations, e.g. for carbon to describe phase transformations in the Fe–C system, and thermodynamic databases, e.g. Thermo-Calc® [8]. Further, elastic strain contributions to the free energy can be considered and the phase field equations can be coupled to temperature equations [1]. Each grain in the simulation domain can be characterized with a number of attributes, e.g. its phase and crystallographic orientation. This leads to a multiplicity of potential interfacial properties (μ_{ij}, σ_{ij}, η_{ij}) that must be provided as an input. The advantage here is that anisotropy in these properties can in principle be incorporated. But it must be noted that exact knowledge of interfacial parameters, in particular mobilities, and their potential anisotropy is rather limited. Since the PFM is derived as a growth model, nucleation of grains with a new phase is another process that must be quantified as input information. PFM simulation results depend markedly on the selected density and distribution of nuclei as well as the rate of nucleation. As a result, interfacial mobilities, anisotropy factors and nucleation scenarios can be employed as adjustable parameters when a quantitative description of experimental observations is sought. In addition, the treatment of the interface region is a critical issue in PFMs because of the diffuse nature of the interface. To reduce computational cost, interface thicknesses employed in simulations can frequently be orders of magnitude larger than the actual interface thickness. Therefore, careful asymptotic analyses are required to make conclusions on the sharp interface limit. Different assumptions for the interface region are available for phase transformations that either consider this region as a mixture of the two phases having the same composition [9] or as a mixture of the two phases with different composition that are defined by a constant ratio for each element [10].

These potential challenges of treating the interface are more than compensated for by the fact that no explicit tracking of the interface is required. Therefore, phase field models provide a powerful methodology to describe phase transformations. This technique can easily handle time-dependent growth geometries, and thus enables the prediction of complex microstructure morphologies making the PFM approach particularly suitable for phase transformations in steels where morphological complexities are common, e.g. for austenite formation as well as austenite decomposition into Widmanstätten ferrite and bainite.

Initially, the application of PFMs emphasized solidification processes to describe dendrite formation. Böttger et al. [1] gave an overview on solidification simulations for steels including solidification in stainless steels, continuous casting and graphite nucleation in cast irons. Another important example is the simulation of the peritectic solidification in Fe–C by Tiaden [11]. A unique phase field application involving liquid steel is the description of scrap melting by Li et al. [3,12] with immediate practical relevance for electric arc furnace (EAF) steelmaking. Solid–liquid transformations may be considered as classical examples that have established the phase field approach as a powerful computational materials science tool, in particular for modeling the formation of dendrites. More recently, the application of PFMs has also emphasized solid–solid transformations starting with the all important transformation of austenite (γ) to ferrite (α).

3. Austenite decomposition

3.1. Transformation modes

A number of important advances have been made in describing the austenite-to-ferrite transformation kinetics with PFMs. Early work on this subject can be traced back about a decade [4,13]. An emphasis of this earlier work was to investigate interfacial conditions and the transition between different transformation modes. Some of these fundamental studies were accomplished with 1D simulations. For example, Yeon et al. [4] analyzed local equilibrium conditions for an Fe–Cr–Ni alloy and para-equilibrium conditions for the Fe–C–Mn system. Loginova et al. [5] developed a PFM and applied it in 1D for binary Fe–C alloys to assess the transition between diffusion controlled and massive transformation. The PFM predicts a transition to the partitionless massive transformation for sufficiently high undercooling in qualitative agreement with experimental observations. Because of the low computational cost of 1D simulations an interface thickness can be employed approaching that of the physical interface – for example 1 nm in the work of Loginova et al. [5].

Loginova et al. [14] extended then their PFM simulations to 2D and considered that the α–γ interfacial energy and the interface thickness depend on the orientation of the growth direction. This anisotropy function was expressed in terms of an amplitude that provides a relationship between maximum and minimum interfacial energies to mimic high-energy incoherent and low-energy coherent interfaces, respectively. As shown in Fig. 1, they were able to predict the growth of Widmanstätten ferrite in an Fe–0.22 wt%C alloy at 720 °C provided a sufficiently large anisotropy amplitude is selected. The value of the critical amplitude increases with decreasing interface thickness and extrapolation to a realistic interface thickness of 1 nm suggested a rather high value of 100 for the investigated condition but the authors indicated that a higher undercooling may lower this critical value. More recently, Yamanaka et al. [15] proposed an alternative approach to introduce anisotropy of the interfacial energy but similarly to Loginova et al. [14] the anisotropy magnitude is described by a strength factor. Simulating isothermal austenite–ferrite transformation in Fe–C the transition from allotriomorphic to Widmanstätten ferrite is predicted with increase in the anisotropy strength, as shown in Fig. 2. A further increase in anisotropy magnitude leads to a refinement of the Widmanstätten structure. The studies by Loginova et al. [5,14] and Yamanaka et al. [15] are excellent examples of

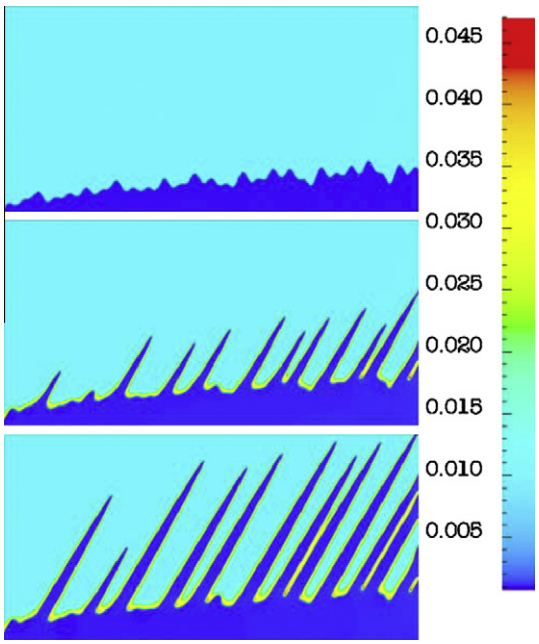

Fig. 1. 2D phase field simulations of Widmanstätten ferrite growth [14]. Colors (grey scale) indicate the carbon concentration level.

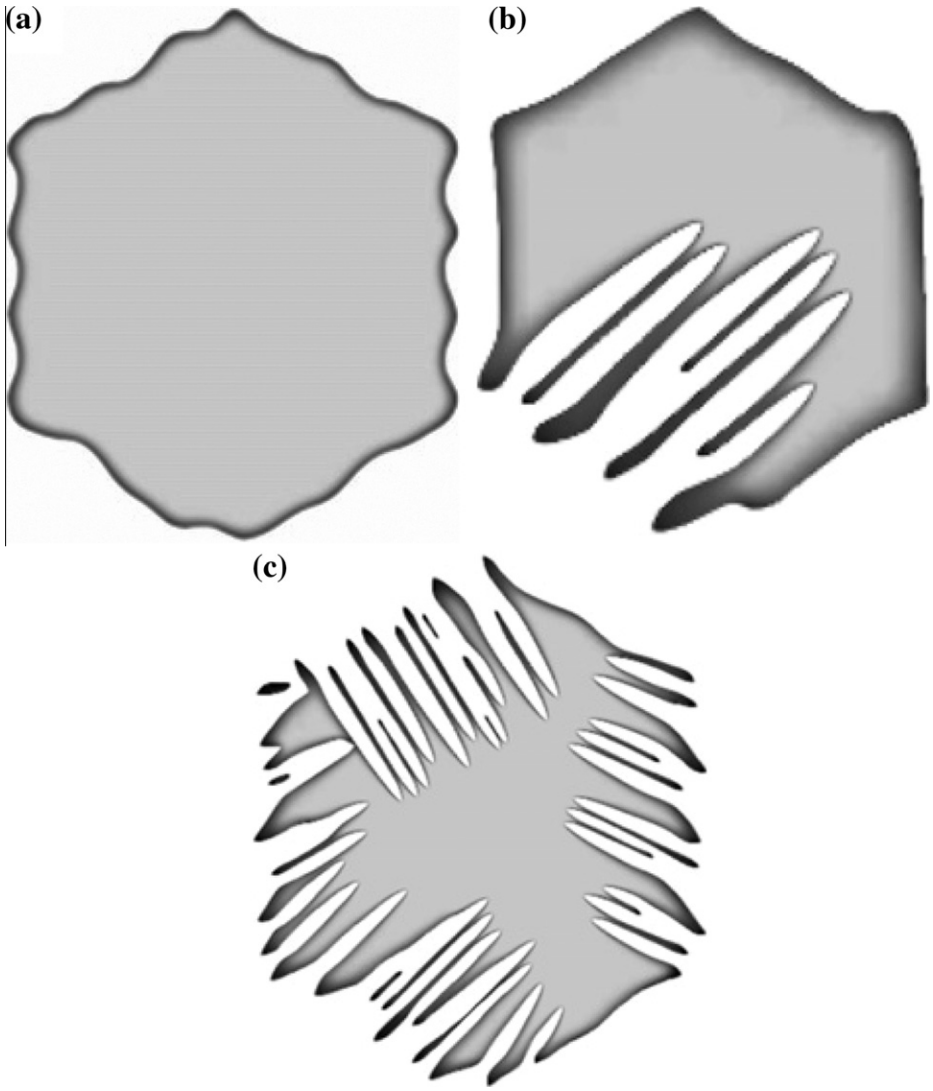

Fig. 2. 2D PFM simulations of ferrite growth into a hexagonal austenite grain surrounded by a ferrite matrix assuming different anisotropy factors (a) 0.1, (b) 0.35, and (c) 0.5 [15].

the potential of PFMs to predict complex transformations from austenite into a number of transformation products, i.e. here polygonal, massive and Widmanstätten ferrite.

Further, the cooperative growth of pearlite from austenite in an Fe–C alloy was simulated with the phase field approach by Nakajima et al. [16]. They selected sufficiently large interfacial mobilities such that pearlite formation is controlled by carbon diffusion and studied systematically the effects of interlamellar spacing and undercooling on the transformation rate. Examples of their 2D simulations are shown in Fig. 3 illustrating that for a very fine spacing with large curvature ferrite overgrows cementite such that a lamellar structure cannot evolve. Medium interlamellar spacing shows the highest growth velocity before the velocity decreases with increasing spacing. Only carbon diffusion in austenite was taken into account in the simulations shown in Fig. 3. Including diffusion in ferrite increased pearlite growth rates by about a factor of 4 but they were still somewhat lower than observed experimentally. To close the gap with the experimental data Steinbach and Apel [17] extended these phase field simulations by considering the effect of strain and stress on the pearlite formation kinetics. According to their analysis transformation strain inhibits the cooperative growth mode of ferrite and cementite but provokes salient

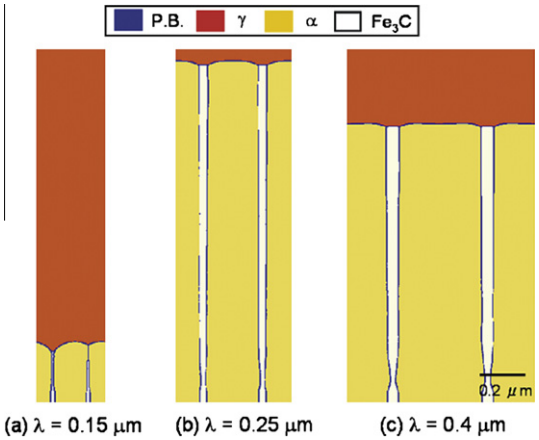

Fig. 3. 2D PFM simulations of austenite-to-pearlite transformation in an Fe–C alloy with different interlamellar spacing assuming that carbon diffusion occurs in austenite only [16].

growth of cementite needles ahead of the ferrite front. This staggered growth mode, i.e. cementite platelets grow into austenite

followed by ferrite within a distance comparable to the width of the cementite lamellae, results in growth velocities that are in agreement with experimental data.

In addition to these diffusional transformations, PFMs were also developed to describe the displacive martensitic transformation albeit no application to steel has been reported so far. However, an Fe-based alloy, i.e. Fe–31%Ni, was considered in 3D simulations of martensite formation [18]. Thus, the potency of PFMs for simulating austenite decomposition has been shown for all but bainitic transformation products. It must, however, be emphasized that the above discussed simulations for the formation of ferrite and pearlite were conducted in 1D and/or 2D starting from an austenite–ferrite dual-phase structure, i.e. no consideration was given to the nucleation stage that one would have to include when simulating the overall transformation.

3.2. Overall transformation kinetics

Pariser et al. [13] were the first who used PFM simulations to describe the overall austenite-to-ferrite transformation assuming that interfacial parameters depend only on the phases of the neighbouring grains, i.e. α–α, α–γ, γ–γ. Conducting 2D simulations they replicated experimentally observed continuous cooling transformation kinetics in two steels with ultra low-carbon content (22 and 33 wt ppm, respectively) by adjusting the interface mobility and selecting a suitable nucleation scenario (undercooling for nucleation, selection of nucleation sites at austenite grain boundaries). Subsequently, Mecozzi et al. [19–21] conducted similar 2D simulations to describe continuous cooling transformation kinetics in low-carbon steels including a Nb microalloyed grade. In these low-carbon steels transformation rates depend also on long range diffusion of carbon and the transformation is of mixed-mode character, i.e. it changes gradually from interface to carbon diffusion controlled [22]. The PFM replicates the mixed-mode philosophy as both interfacial reaction and carbon diffusion are included into the simulations – the much slower redistribution of substitutional alloying elements is usually not considered and para-equilibrium is then frequently assumed to determine the driving pressure for the transformation.

A particular drawback of these austenite–ferrite phase field models is that they are 2D simulations. First 3D simulations of the austenite-to-ferrite transformation were recently conducted by Militzer et al. [23]. As shown in Fig. 4, 3D simulations lead to much more realistic microstructures as compared to 2D simulations. From a morphological point of view realistic grain shapes are apparent in the 2D cuts from 3D simulations whereas in 2D simulations unrealistic grain shapes frequently result, e.g. the remaining austenite develops long-elongated channels with a number of narrow inlet-type features between ferrite grains that often appear as squished circles (see Fig. 4c). Further, the role of nucleation behavior was analyzed in detail with these 3D simulations [23]. Primarily, the α–γ interface mobility, μ, was used to fit experimentally observed transformation kinetics. However, the selection of the mobility values depends on the assumed nucle-

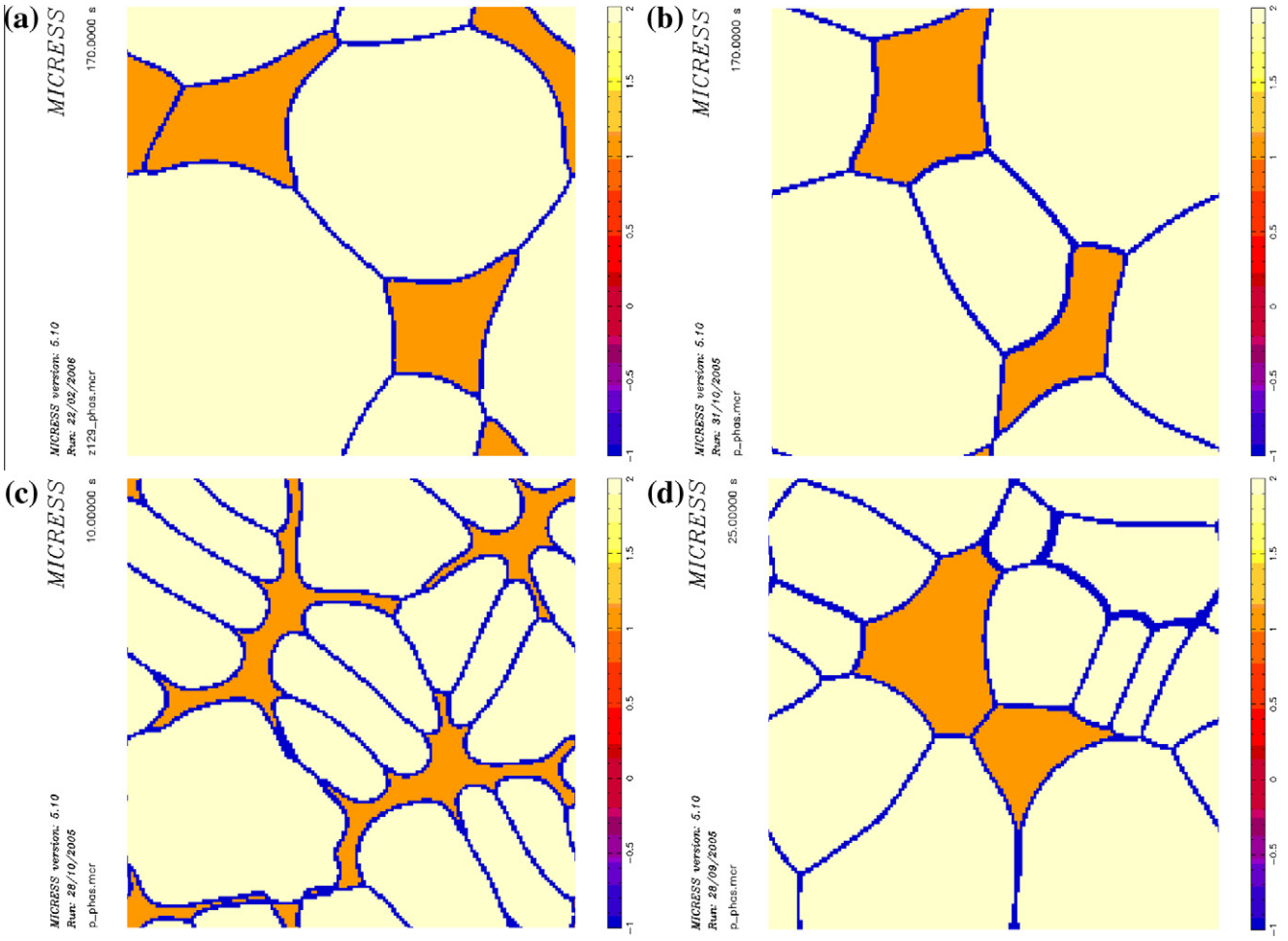

Fig. 4. Comparison of PFM simulated 2D (left) vs. 3D (right) microstructures for continuous cooling transformation in a 0.1 wt%C–0.49 wt%Mn steel at 0.4 °C/s (top) and 10 °C/s (bottom); ferrite (white), austenite (orange/grey), interfaces (blue/dark) [23].

ation scenario (nuclei density, spatial distribution of nuclei, nucleation temperature range). The analysis by Mecozzi et al. [24] used the ferrite grain size distribution to determine a likely nucleation scenario. In their simulations all nuclei form at the austenite grain boundary with triple lines as preferred nucleation sites and each nucleus leads to a ferrite grain in the final microstructure by assuming sufficiently small grain boundary mobilities. The nuclei density determines the average grain size while the temperature range, δT, of nucleation determines the width of the grain size distribution. This approach permits one to discriminate which of the μ–δT combinations best replicate the experimental (or reference) transformation kinetics. A concern in this approach is that simulations are carried out without accounting for ferrite grain coarsening. Huang et al. [6,25] presented a 2D phase field model that deals with the austenite-to-ferrite transformation and includes also ferrite growth. Substantial ferrite grain coarsening occurred in their simulations of continuous cooling transformation in a 0.17 wt%C–0.74 wt%Mn steel – about 50 pct of the nuclei have been consumed at the completion of transformation [6]. Both grain growth and grain coalescence contributed to grain coarsening in these simulations. To account for coalescence an additional equation was introduced that includes a mobility of ferrite grain rotation. The assumption that not all nuclei will lead to a ferrite grain in the final microstructure is very reasonable but extensive experimental investigations would be required to justify the selection of suitable mobility parameters for the ferrite grains. Further, Huang et al. [6] suggested that for sufficiently fast cooling nucleation sites in the grain interior are also activated, see Fig. 5.

As described above, a number of approaches have been proposed for the introduction of ferrite nuclei into the simulation domain. There are multiplicities of nucleation parameters that can, at least in part, be estimated from experimental data. Some of these parameters seem to be more qualitatively motivated (e.g. not all nuclei will survive the transformation) whereas others (e.g. nucleation temperature range δT) have a more quantitative grounding with experimental data. Overall, however, the selection of the α–γ interface mobility remains a crucial issue that has yet to be resolved satisfactorily using fundamental studies that may include atomistic simulations. In the PFM simulations interface mobilities are adopted as effective values. In the simulations of Mecozzi et al. [19–21,24] and Militzer et al. [23] an Arrhenius relationship was assumed for the temperature dependence of the mobility with a generally accepted activation energy of 140 kJ/mol. Then, just the pre-exponential mobility factor was employed as an adjustable parameter and it was found that this factor increases with cooling rate. Simulating continuous cooling transformation in an Fe–0.1 wt%C–0.49 wt%Mn alloy Militzer et al. [23] suggested an increase of the pre-exponential mobility term by a factor of approximately 7 when the average transformation temperature decreases by about 70 °C as a result of increasing the cooling rate from 0.4 to 10 °C/s. Similarly, Huang et al. [6,25] introduced a correction term to the Arrhenius relationship of the interface mobility. Their correction term decreases linearly with increasing temperature.

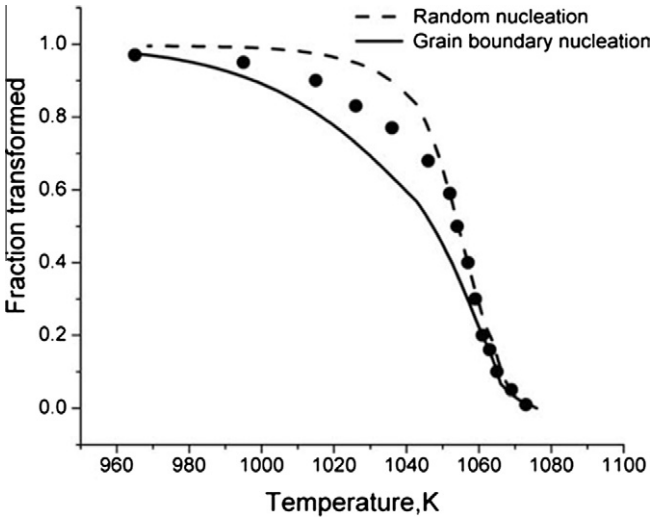

Fig. 5. Role of nucleation site selection on PFM prediction of ferrite formation in a 0.17 wt%C–0.74 wt%Mn steel cooled at 53 °C/s [6].

In essence, physical models are required to account for this temperature trend of the effective mobility. Takahama and Sietsma [26] provided an attempt to analyze the mobility term obtained in 2D and 3D simulations for austenite-to-ferrite transformation in a Nb microalloyed steel (0.136 wt%C–1.2 wt%Mn–0.02 wt%Nb) cooled at 0.3 °C/s from different austenitization temperatures ranging from 900 to 1200 °C. Increasing the austenitization temperature increases the austenite grain size and thus lowers the transformation temperature. Using the aforementioned procedures [19–21,23,24] the pre-exponential mobility values were adjusted and found to increase with decreasing transformation temperature. This trend was then rationalized in terms of solute drag and pinning by NbC. The amount of Nb in solution increases with reheating temperature, as experimentally quantified for the investigated case. Even so, de-convolution of the effects of pinning and solute drag on the effective mobility remains a challenge. To obtain an interpretation of their mobility values Takahama and Sietsma [26] suggested a decrease of solute drag for the highest reheating temperature of 1200 °C because of the higher velocity values that are observed for this case with the lowest transformation temperature. Solute drag depends on the velocity of the interface but a more rigorous evaluation of this dependency could not be included in the proposed analysis. As a result, all these phase field models appear to be descriptive and have yet to be brought to a stage that reliable quantitative predictions can be made for commercial steels.

Nevertheless, application of the PFM methodology to advanced high strength steels is progressing. For example, Suwanpinij et al. [27] used 2D PFM simulations to describe the decomposition of pancaked, i.e. non-recrystallized, austenite in a dual-phase steel (0.073 wt%C–1.43 wt%Mn–0.13 wt%Mo) with different levels of applied strain up to 0.6. The simulations were carried out for isothermal transformation at 680 °C and compared with experimental data. Mobility values, nuclei densities and the sequence of introducing nuclei during the transformation were selected such that transformation kinetics and ferrite grain size distributions at intermediate transformation stages were in reasonable agreement with experimental observations. Three nucleation sites were considered, i.e. grain corners/edges, grain boundary faces and bulk. The magnitude of nucleation at less favorable sites, i.e. grain faces and in the bulk, increases with applied strain (i.e. increased degree of pancaking). Thiessen et al. [28] performed 2D phase field simulations for ferrite formation during continuous cooling at 10 °C/s from a fully austenitic and a partially austenitic, i.e. intercritical structure in another dual-phase steel (0.09 wt%C–1.72 wt%Mn–0.26 wt%Si). Their consideration of introducing nuclei employed classical nucleation theory with at least six empirical parameters to capture nucleation at three different grain boundary sites (corners, edges, faces) – an approach they had first proposed for simulating phase transformations in a plain low-carbon steel (0.05 wt%C–0.31 wt%Mn–0.18 wt%Si) [29]. The geometric factor representing the potency of the nucleation sites, i.e. the difference of added and removed interfacial energy, was adopted using literature values. The densities of these nucleation sites were determined similar to the procedures proposed by Mecozzi et al. [19–21,24] to replicate the final ferrite grain size. Further, selecting suitable mobility terms with an activation energy of 160 kJ/mol

enabled the experimentally observed transformation rates to be described. The simulated microstructures compare favorably to those observed experimentally, as shown in Fig. 6.

An interesting attempt to use PFM simulations was recently made to gain insight into phase transformation mechanisms in advanced steels for the new quenching and partitioning (Q&P) heat treatment route [30]. The Q&P process was simulated for a low-carbon–high-aluminum steel. Starting with a partially austenitized microstructure that is inferred from the as-received microstructure of the steel epitaxial ferrite growth and carbon redistribution were simulated during rapid cooling at 100 °C/s to the quench temperature below the martensite start temperature. Using an activation energy of 140 kJ/mol, the pre-exponential terms of the interfacial mobilities were determined to obtain agreement of simulated microstructures with those observed after quenching. Based on the carbon content and the quench temperature the austenite portions were assigned that remain as austenite and transform to martensite, respectively. Subsequently, the carbon partitioning step at 350 °C was simulated concluding that depending on the quench temperature austenite may either grow or shrink. The formation of bainite was not included in these initial Q&P simulations even though there is experimental evidence that bainite forms during the partitioning step.

4. Austenite formation

Compared to austenite decomposition the reverse transformation, i.e. austenite formation, has been much less studied. This is mirrored by the status of PFM simulations of these two transformations. Only some very initial PFM studies have been reported on austenite formation [28,29,31–34]. Thiessen et al. [28,29] employed 2D phase field modeling to investigate austenite formation from ferrite–pearlite and ferrite–martensite structures during heat treatment cycles that are similar to those in the weld HAZ. However, to reduce computational cost they simplified pearlite as supersaturated ferrite with eutectoid carbon content and without resolving the carbide lamellae. Building on this approach, Savran [32] described austenite formation during continuous heating in a number of carbon steels (0.2–0.6 wt%C). Adjusting the interface mobilities agreement with experimentally observed transformation kinetics was obtained. For very slow heating (0.05 °C/s) a mobility value was employed that is a factor 10 lower than for more rapid heating (3 °C/s). This finding was explained with potential spheroidization of pearlite and/or Mn redistribution during very slow heating. The selected mobilities are consistent with a mixed-mode character for austenite formation.

Savran [32] also attempted very preliminary simulations of intercritical austenite formation taking explicitly into account the lamellar pearlite structure. However, some of the physical parameters such as interfacial energies used in the model were unrealistic, e.g. 0.039 J/m^2 for the ferrite/austenite interface. Using more realistic values for interfacial energies, Azizi-Alizamini and Militzer [33,34] simulated austenite formation in the Fe–C system using ultrafine ferrite–cementite aggregates, pearlite and ferrite–pearlite as initial microstructures. First, they benchmarked their 2D simulations for isothermal conditions with models for long range carbon diffusion controlled austenite formation kinetics by using a sufficiently large interface mobility. Then, they applied this model to the pearlite-to-austenite formation in a pearlitic steel and confirmed experimental observations in terms of growth rates and morphologies [34]. In particular, preferential growth of austenite along cementite lamellae is predicted and austenite growth rates are sufficiently large that partially undissolved cementite particles remain temporarily within the austenite matrix. As illustrated in Fig. 7, these general morphological aspects were also predicted

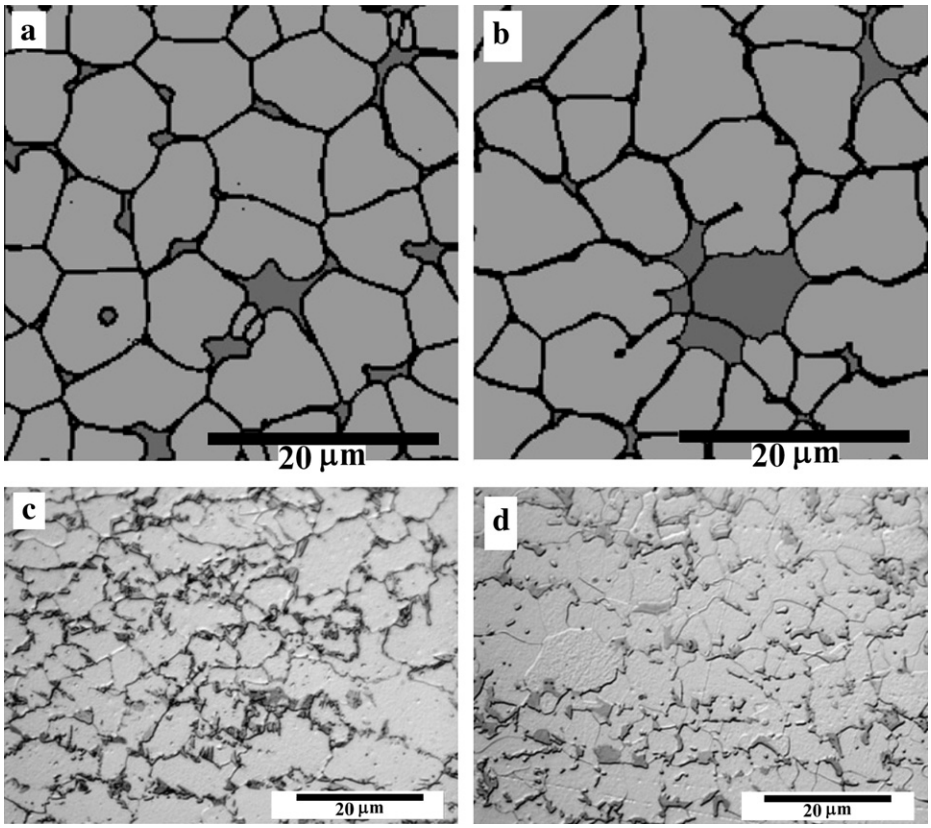

Fig. 6. Comparison of simulated and metallographically observed microstructures in a 0.09 wt%C–1.72 wt%Mn–0.26 wt%Si steel cooled at 10 °C/s after full austenitization (a and c) and intercritical austenitization (b and d) [28].

when simulating austenite formation from a ferrite–pearlite microstructure in an Fe–0.17 wt%C alloy intercritically annealed at 750 °C. The resulting finger-type morphology of intercritical austenite is consistent with experimental observations [32]. These simulations also confirmed rapid pearlite-to-austenite transformation that is followed by the much slower ferrite-to-austenite transformation. These predictions were similar to those made by Savran [32]. Further, a systematic PFM study was conducted for intercritical austenite formation from ultrafine ferrite–cementite aggregates with circular (2D) and spherical particles (3D) in the diffusion controlled limit [33]. The model was capable of resolving carbide particle sizes of about 100 nm to simulate the morphological complexity during austenite formation. A representative simulation result is shown in Fig. 8. There is a tendency of preferential growth of austenite towards carbides as the sources of carbon for austenite growth again resulting in the development of finger-type structures. The degree of these morphological aspects depends significantly on spacing and distribution of cementite particles that provide suitable nucleation sites for austenite. Further, there is a trend for rapid coarsening of the austenite grains (see Fig. 8c and d) due to curvature effects and short diffusion distances.

These simulation results provide insight into the evolution of austenite–ferrite dual-phase structures during intercritical annealing of advanced high strength steels. However, because of the morphological complexity it is of paramount importance to complete a series of 3D simulations to assess the validity of the 2D simulations. Azizi-Alizamini and Militzer provided just one 3D simulation result of austenite formation from spherical cementite particles [33]. Further, to obtain a quantitative description of austenite formation in advanced high strength steels the role of substitutional alloying elements needs to be incorporated into PFM simulations. The challenge is similar to what has been discussed above for austenite decomposition. It can be expected that the effective mobility approach utilized by Thiessen et al. [28,29] and Savran [32] in their austenite formation simulations adopting homogenized pearlite will be employed in future simulations incorporating the lamellar pearlite structure. Subsequently, these mobility values and their temperature dependence can be rationalized with more physically based models.

5. Recrystallization and grain growth

PFMs can readily be used to simulate recrystallization and grain growth. The chemical driving pressure in Eq. (1) is replaced by the stored energy for recrystallization simulations whereas it is simply zero for grain growth. Sophisticated phase field model procedures have been proposed to simulate static and dynamic recrystallization [35–37] as well as grain growth including abnormal grain growth [38–40] and the role of particle pinning [41–43] has been considered. Most PFM models that include pinning resolve the particles explicitly in the simulation mesh thereby limiting their applicability to situations where particle spacing and grain size are comparable (e.g. nanocrystalline materials, pinning by relatively coarse TiN particles in steels). Further, these simulations must be performed in 3D to permit a meaningful comparison with experimental data. Recently Apel et al. [44] suggested including the role of pinning into a driving pressure dependent effective mobility – the mobility value reaches zero when the driving pressure at a given boundary is compensated by the assumed pinning pressure. Alternatively, Shahandeh and Militzer [45] proposed a method to introduce a friction pressure that is equal to the pinning pressure to simulate particle pinning without resolving particles explicitly. This approach may also be useful to efficiently incorporate solute drag into phase field simulations but in this case the friction pressure will also have to be a suitable function of interface velocity.

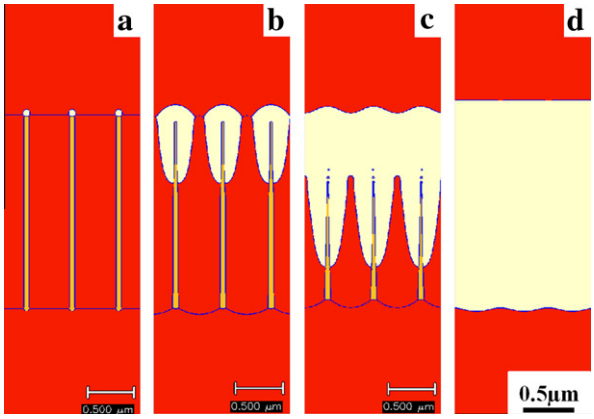

Fig. 7. Phase field simulation of austenite formation in Fe–0.17 wt%C at an intercritical annealing temperature of 750 °C: (a) initial ferrite–pearlite structure with austenite nuclei, (b) 0.05 s, (c) 0.1 s, (d) 0.25 s; (ferrite: red/dark grey, cementite: yellow/light grey, austenite: white, interfaces: blue/black) [34].

The application of these PFMs to recrystallization and grain growth in steels is rather limited so far. The aforementioned austenite-to-ferrite transformation simulations by Huang et al. [6,25] can be viewed as an example for grain growth simulations since ferrite grain coarsening was explicitly considered. Thiessen and Richardson [46] performed 2D simulations of recrystallization and grain growth in an austenitic stainless steel for heat treatment cycles that are typical for a number of positions in the HAZ of welds. Selecting a distribution of stored energy among different grains and suitable nucleation densities they were able to reproduce the grain size distribution as a function of position from the weld. Lefebvre et al. [47] used 2D simulations with a homogeneous distribution of the stored energy but a spatially non-uniform nuclei distribution, i.e. there are layers without nuclei embedded in a matrix with randomly distributed nuclei, to rationalize a two-stage recrystallization behavior observed in a ferritic stainless steel.

Phase field simulations of austenite grain growth have recently gained momentum with the goal of predicting microstructure evolution in the HAZ. Even though the work of Thiessen et al. [28,29,46] was aimed at simulating the microstructure at selected positions in the HAZ, their approach was to adopt the time–temperature profile for these positions but otherwise to assume a homogeneous temperature throughout the simulation domain, i.e. in essence microstructure evolution was simulated for a bulk sample subjected to the selected heat treatment cycle. One of the advantages of PFM is, however, that the spatially steep temperature gradient, i.e. on the length scale of a few grains, can readily be incorporated into the simulations. Toloui and Militzer [48,49] have recently initiated a series of dedicated simulations of austenite grain growth in the HAZ of a Nb–Ti microalloyed low-carbon steel. Using experimental data for austenite grain growth during continuous heating in bulk samples they determined the effective grain boundary mobility as a function of temperature assuming ideal grain growth [48]. In this steel, grain growth is affected by particle pinning due to NbC and TiN. Nevertheless, the authors argued that an explicit consideration of pinning is not required because of the very rapid heat treatment cycles of a few seconds. The effective mobility then becomes a complex function of temperature as the pinning pressure decreases with increasing temperature due to dissolution of NbC. Two Arrhenius relationships were proposed for the mobility – one for the strong pinning at lower temperature and another one for the weak pinning at higher temperatures. These two mobility branches are separated by a gradual transition for intermediate temperatures where NbC dissolves. Using these mobility terms, Toloui and Militzer replicated experi-

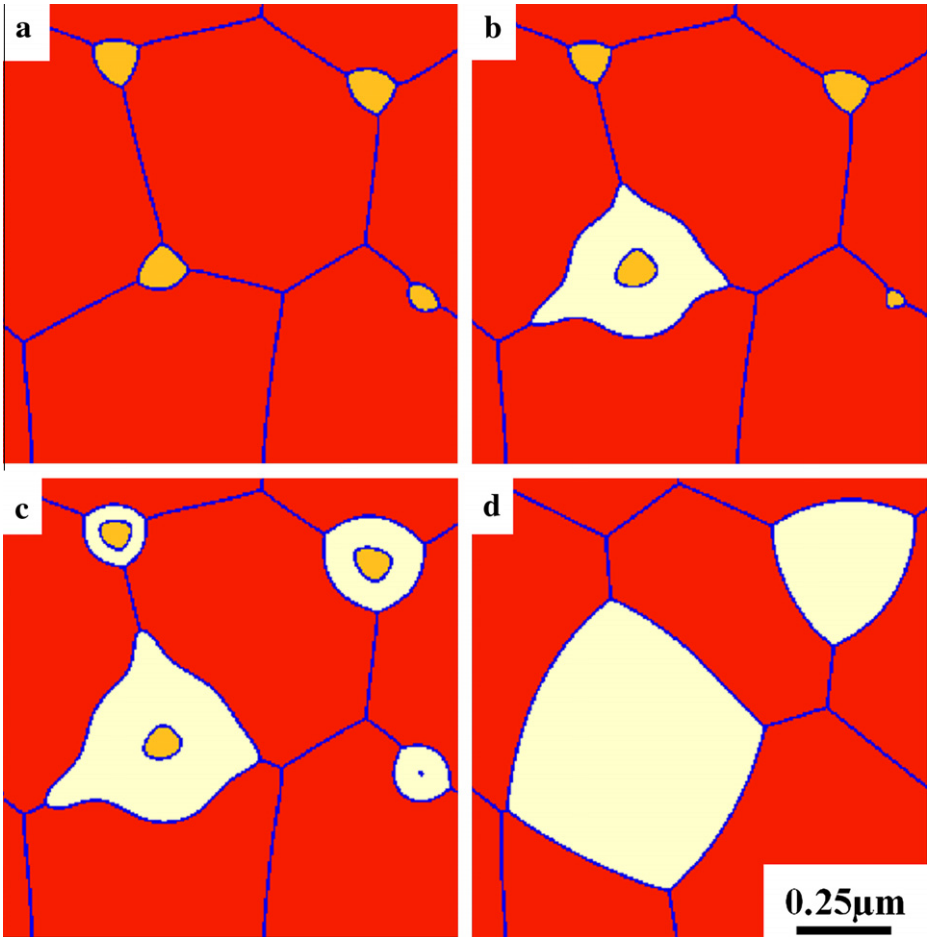

Fig. 8. Evolution of austenite from an ultrafine grained ferrite–cementite aggregate at 750 °C in Fe–0.17 wt%C: (a) initial structure, (b) 0.02 s, (c) 0.03 s, (d) 5 s (ferrite: red/dark grey, cementite: yellow/light grey, austenite: white, interfaces: blue/black) [33].

mental observations of austenite grain growth for a wide range of different rapid heat treatments with their 2D and 3D phase field simulations, as illustrated with the example shown in Fig. 9. They also showed that 2D and 3D simulations give essentially the same result provided the effective mobility in the 3D simulations is a factor 0.7 smaller than in the 2D simulations [49]. Similar 2D vs. 3D mobility considerations were made for the α - γ transformation [23] and could be rationalized by the underlying growth geometries – 2D calculations represent cylindrical growth in 3D whereas 3D simulations for equiaxed features are more consistent with spherical growth. Using 2D simulations Toloui and Militzer extended their austenite grain growth modeling to the actual situation of the HAZ with steep temperature gradients [48]. The simulations were performed by splitting the HAZ into a number of simulation domains. In each domain a linear temperature gradient was assumed as a function of position, i.e. from the left to the right side of the domain. The left and right boundaries experience the representative time–temperature profile for these particular positions in the HAZ. As illustrated in Fig. 10, semi-quantitative agreement was obtained with the grain structures observed as a

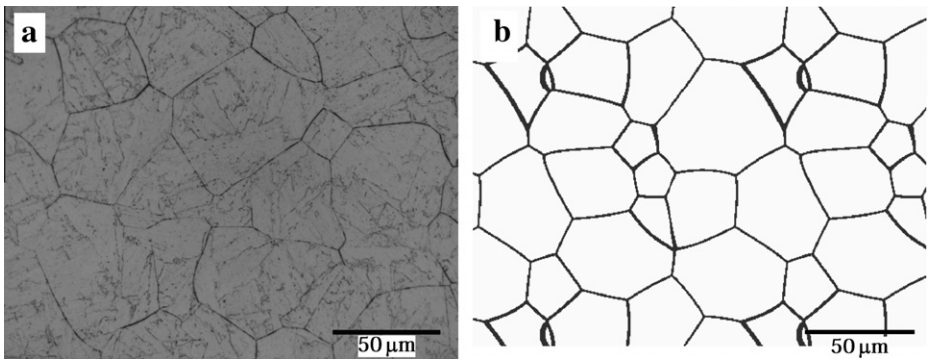

Fig. 9. Non-isothermal austenite grain growth in a Nb–Ti microalloyed linepipe steel heated at 1000 °C/s to 1350 °C and cooled at 100 °C/s to 900 °C: (a) experimental observation of Banerjee et al. [50], (b) representative 2D cut of 3D phase field simulation [49].

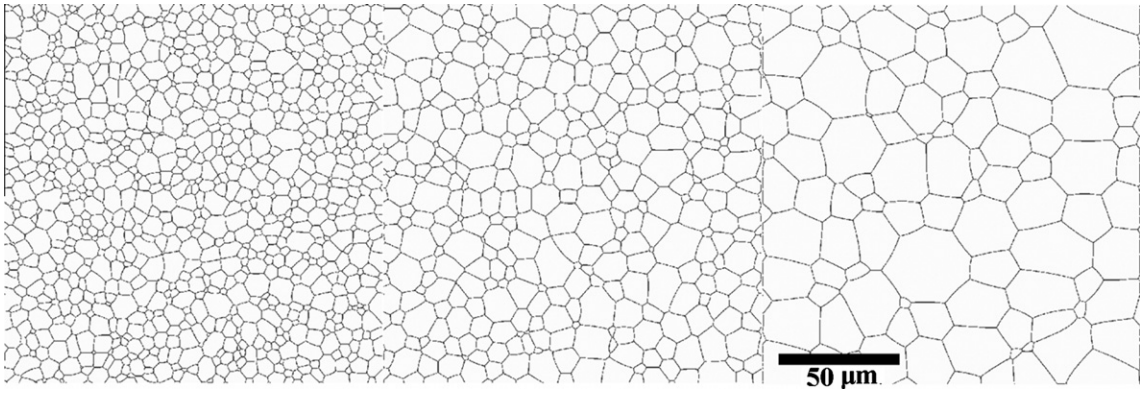

Fig. 10. 2D phase field simulation of austenite grain growth in the HAZ of a Nb–Ti microalloyed linepipe steel [48].

function of the position from the fusion line. Again this is an excellent example of the power of phase field models to describe and potentially to predict complex microstructure evolution scenarios – after benchmarking the mobilities with data from bulk samples no further fit parameters were employed in the HAZ simulations. It will only be a matter of time that more efficient and elegant PFM simulations for the HAZ will be conducted adopting non-linear temperature gradients directly within the calculation domain.

6. Conclusions

Overall, PFMs are a very promising tool for the modeling of the microstructure evolution in steels. A particular advantage of the PFM approach is that one modeling tool can be used to track the microstructure evolution from casting to the final processing step, e.g. either coiling or annealing for sheet production. A particular strength of the phase field approach is that morphologically complex features can be readily simulated, as e.g. illustrated for Widmanstätten ferrite. The only transformation product that has yet to be considered with phase field modeling is bainite which may not be surprising given the complexity of the bainite reaction that is still controversially discussed as either displacive or diffusional transformation. The progress in applying phase field models to advanced high strength steels must be seen as an indication that initial bainite phase field simulations will be presented in the near future. It is likely that these first attempts will be built on the approach used for modeling Widmanstätten ferrite, i.e. suitable anisotropic interfacial properties may be assumed.

Further, PFM simulations are well suited for situations where different microstructure processes occur simultaneously, e.g. spheroidization, recrystallization and austenite formation during annealing of cold-rolled steels. A limitation here may be the potentially different length scales of individual microstructure processes. Important examples for steels in this regard are grain growth pinned by nano-sized precipitates and the pearlite-to-austenite formation where the lamellar pearlite structure has a much smaller length scale than the austenite grains. To bridge these length scales suitable approximations, e.g. describing pearlite as ferrite with eutectoid carbon concentration [28,29,32], can be used in the PFM simulations rather than employing a more rigorous, but computational expensive approach. Interfacial parameters and nucleation scenarios are crucial input information that is frequently used in an empirical way to fit experimental observations thereby limiting the predictive capability of the PFM approach. Nevertheless, PFM simulations can provide invaluable qualitative and semi-quantitative insight into phase transformation mechanisms in steels with complex microstructural morphologies.

Acknowledgement

It is a pleasure to acknowledge the assistance of Chad Sinclair, Hamid Azizi-Alizamini, Morteza Toloui, Sina Shahandeh, Benqiang Zhu and Michael Greenwood in finalizing this review paper.

References

[1] Böttger B, Apel M, Eiken J, Schaffnit P, Steinbach I. Phase-field simulation of solidification and solid–solid transformations in multicomponent steels. Steel Res Int 2008;79:608–16.
[2] <http://www.access.rwth-aachen.de/MICRESS/>.
[3] Li J, Brooks G, Provatas N. Kinetics of scrap melting in liquid steel. Metall Mater Trans B 2005;36B:293–302.
[4] Yeon DH, Cha PR, Yoon JK. A phase field study for ferrite–austenite transitions under para-equilibrium. Scripta Mater 2001;45:661–8.
[5] Loginova I, Odqvist J, Amberg G, Ågren J. The phase-field approach and solute drag modeling of the transition to massive γ–α transformation in binary Fe–C alloys. Acta Mater 2003;51:1327–39.
[6] Huang CJ, Browne DJ, McFadden S. A phase-field simulation of austenite to ferrite transformation kinetics in low carbon steels. Acta Mater 2006;54:11–21.
[7] Steinbach I, Pezzola F, Nestler B, Seeßelberg M, Prieler R, Schmitz GJ, et al. A phase field concept for multiphase systems. Physica D 1996;94:135–47.
[8] <http://www.thermocalc.com>.
[9] Wheeler AA, Boettinger WJ, McFadden GB. Phase-field model for isothermal phase-transitions in binary-alloys. Phys Rev A 1992;45:7424–39.
[10] Tiaden J, Nestler B, Diepers HJ, Steinbach I. The multiphase-field model with an integrated concept for modelling solute diffusion. Physica D 1998;115:73–86.
[11] Tiaden J. Phase field simulations of the peritectic solidification of Fe–C. J Cryst Growth 1999;198/199:1275–80.
[12] Li J, Provatas N. Kinetics of scrap melting in liquid steel: multipiece scrap melting. Metall Mater Trans B 2008;39B:268–79.
[13] Pariser G, Shaffnit P, Steinbach I, Bleck W. Simulation of the γ–α transformation using the phase-field method. Steel Res 2001;72:354–60.
[14] Loginova I, Ågren J, Amberg G. On the formation of Widmanstätten ferrite in binary Fe–C – phase-field approach. Acta Mater 2004;52:4055–63.
[15] Yamanaka A, Takaki T, Tomita Y. Coupled simulation of microstructural formation and deformation behavior of ferrite–pearlite steel by phase-field method and homogenization method. Mater Sci Eng A 2008;480:244–52.
[16] Nakajima K, Apel M, Steinbach I. The role of carbon diffusion in ferrite on the kinetics of cooperative growth of pearlite: a multi-phase field study. Acta Mater 2006;54:3665–72.
[17] Steinbach I, Apel M. The influence of lattice strain on pearlite formation in Fe–C. Acta Mater 2007;55:4817–22.
[18] Artemev A, Jin Y, Khachaturyan AG. Three-dimensional phase field model of proper martensitic transformation. Acta Mater 2001;49:1165–77.
[19] Mecozzi MG, Sietsma J, van der Zwaag S. Phase field modelling of the interfacial condition at the moving interphase during the $\gamma \rightarrow \alpha$ transformation in C–Mn steels. Comput Mater Sci 2005;34:290–7.
[20] Mecozzi MG, Sietsma J, van der Zwaag S, Apel M, Schaffnit P, Steinbach I. Analysis of the $\gamma \rightarrow \alpha$ transformation in a C–Mn steel by phase field modeling. Metall Mater Trans A 2005;36A:2327–40.
[21] Mecozzi MG, Sietsma J, van der Zwaag S. Analysis of $\gamma \rightarrow \alpha$ transformation in a Nb micro-alloyed C–Mn steel by phase field modelling. Acta Mater 2006;54:1431–40.
[22] Sietsma J, van der Zwaag S. A concise model for mixed-mode phase transformations in the solid state. Acta Mater 2004;52:4143–52.

[23] Militzer M, Mecozzi MG, Sietsma J, van der Zwaag S. Three-dimensional phase field modelling of the austenite-to-ferrite transformation. Acta Mater 2006;54:3961–72.
[24] Mecozzi MG, Militzer M, Sietsma J, van der Zwaag S. The role of nucleation behavior in phase-field simulations of the austenite to ferrite transformation. Metall Mater Trans A 2008;39A:1237–47.
[25] Huang CJ, Browne DJ. Phase-field model prediction of nucleation and coarsening during austenite/ferrite transformation in steels. Metall Mater Trans A 2006;37A:589–98.
[26] Takahama Y, Sietsma J. Mobility analysis of the austenite to ferrite transformation in Nb microalloyed steel by phase field modelling. ISIJ Int 2008;48:512–7.
[27] Suwanpinij P, Rudnizki J, Prahl U, Bleck W. Investigation of the effect of deformation on $\gamma \rightarrow \alpha$ transformation kinetics in hot-rolled dual phase steel by phase field approach. Steel Res Int 2009;80:616–22.
[28] Thiessen RG, Sietsma J, Palmer TA, Elmer JW, Richardson IM. Phase-field modelling and synchrotron validation of phase transformations in martensitic dual-phase steel. Acta Mater 2007;55:601–14.
[29] Thiessen RG, Richardson IM, Sietsma J. Physically based modelling of phase transformations during welding of low-carbon steel. Mater Sci Eng A 2006;427:223–31.
[30] Santofimia MJ, Takahama Y, Zhao L, Sietsma J. Analysis of the quenching and partitioning (Q&P) process with partial austenitisation in a low-carbon steel by phase field modelling. In: New developments on metallurgy and applications of high strength steels. Warrendale: TMS; 2008. p. 777–86.
[31] Cordonier J, Militzer M, Jacot A. A phase-field study of the ferrite-to-austenite transformation kinetics. In: Howe JM, Laughlin DE, Lee JK, Dahmen U, Soffa WA, editors. Solid → solid phase transformations in inorganic materials. Warrendale: TMS; 2005. p. 735–40.
[32] Savran VI. Austenite formation in C–Mn steel. PhD thesis, TU Delft; 2009.
[33] Azizi-Alizamini H, Militzer M. Phase field modelling of austenite formation from ultrafine ferrite-carbide aggregates in Fe–C. Int J Mater Res 2010;101:534–41.
[34] Azizi-Alizamini H, Militzer M. Phase field modelling of austenite formation in low-carbon steels. Solid State Phen (special issue – proceedings of PTM 2010). in press.
[35] Takaki T, Tomita Y. Static recrystallization simulations starting from predicted deformation microstructure by coupling multi-phase-field method and finite element method based on crystal plasticity. Int J Mech Sci 2010;52:320–8.
[36] Suwa Y, Saito Y, Onodera H. Phase-field simulation of recrystallization based on the unified subgrain growth theory. Comput Mater Sci 2008;44:286–95.
[37] Takaki T, Hisakuni Y, Hirouchi T, Yamanaka A, Tomita Y. Multi-phase-field simulations for dynamic recrystallization. Comput Mater Sci 2009;45:881–8.
[38] Suwa Y, Saito Y, Onodera H. Three-dimensional phase field simulation of the effect of anisotropy in grain-boundary mobility on grain growth kinetics and morphology of grain structure. Comput Mater Sci 2007;40:40–50.
[39] Ko KJ, Cha PR, Srolovitz D, Hwang NM. Abnormal grain growth induced by sub-boundary-enhanced solid-state wetting: analysis by phase-field simulations. Acta Mater 2009;57:838–45.
[40] Kim SG, Park YB. Grain boundary segregation, solute drag and abnormal grain growth. Acta Mater 2008;56:3739–53.
[41] Suwa Y, Saito Y, Onodera H. Phase field simulation of grain growth in three dimensional system containing finely dispersed second-phase particles. Scripta Mater 2006;55:407–10.
[42] Moelans N, Blanpain B, Wollants P. Pinning effect of second-phase particles on grain growth in polycrystalline films studied by 3-D phase field simulations. Acta Mater 2007;55:2173–82.
[43] Chang K, Feng W, Chen LQ. Effect of second-phase particle morphology on grain growth kinetics. Acta Mater 2009;57:5229–36.
[44] Apel M, Böttger B, Rudnizki J, Schaffnit P, Steinbach I. Grain growth simulations including particle pinning using the multiphase-field concept. ISIJ Int 2009;49:1024–9.
[45] Shahandeh S, Militzer M. Modelling of particle pinning in dual scale using phase field method. In: Proceedings of ReX&GG IV. in press.
[46] Thiessen RG, Richardson IM. A physical based model for microstructure development in a macroscopic heat-affected zone: grain growth and recrystallization. Metall Mater Trans B 2006;37B:655–63.
[47] Lefebvre G, Shahandeh S, Sinclair CW, Militzer M, Mithieux JD, Laigo J. Spatially inhomogeneous recrystallization in ferritic stainless steels. In: Proceedings of ReX&GG IV. in press.
[48] Toloui M, Militzer M. Phase field simulation of austenite grain growth in the HAZ of microalloyed linepipe steel. Int J Mater Res 2010;101:542–8.
[49] Toloui M, Militzer M. 3D phase field simulation of austenite grain growth in microalloyed linepipe steel. In: Proceedings of ReX&GG IV. in press.
[50] Banerjee K, Militzer M, Perez M, Wang X. Nonisothermal austenite grain growth kinetics in a microalloyed X80 linepipe steel. Metall Mater Trans A 2010;41A:3161–72.